Virologica Sinica 41 (2026) 474–477

Contents lists available at ScienceDirect

Virologica Sinica

journal homepage: www.keaipublishing.com/en/journals/virologica-sinica
www.virosin.org

Letter

Identification and characterization of a novel ulcerative enteritis-associated adenovirus of quail causing cross-species infection in chickens

Hui Tang [1], Yin Shi [1], Qing Zhang, Fei Zhu, Jia-Yao Hou, Jing-Ying Liao, Yi-Shuai Zhang, Chang-Xin Jing, Xin-Qi Liu, Chao-Ting Xiao [*]

College of Biology, Hunan Provincial Key Laboratory of Medical Virology, Hunan Research Center of the Basic Discipline for Cell Signaling, Hunan University, Changsha 410082, China

Dear Editor,

The *Adenoviridae* family comprises non-enveloped, icosahedral viruses with linear double-stranded DNA genomes (25–48 kb). Members of this family infect diverse vertebrate hosts, including fish, amphibians, reptiles, birds, and mammals (https://ictv.global/report/chapter/adenoviridae/adenoviridae) (Benko et al., 2022). The *Adenoviridae* family currently comprises more than 260 species classified into six genera *Aviadenovirus*, *Barthadenovirus*, *Ichtadenovirus*, *Mastadenovirus*, *Siadenovirus*, and *Testadenovirus*. Host specificities are genus-dependent: *Mastadenovirus* primarily infects mammals, *Aviadenovirus* primarily infects birds, *Ichtadenovirus* contains a single fish-infecting adenovirus, *Testadenovirus* occurs in turtles, and *Barthadenovirus* (formerly *Atadenovirus*) occurs in squamate reptiles, birds, ruminants, marsupials, and tortoises. *Siadenovirus* infects birds, frogs, and tortoises (https://ictv.global/report/chapter/adenoviridae/adenoviridae). Adenovirus infections exhibit a broad spectrum of severity, ranging from subclinical to lethal.

Members of genus *Siadenovirus* differ substantially from other adenovirus genera both phylogenetically and serologically (Harrach et al., 2019). They share core genomic features with other adenoviruses but possess the shortest genome, characterized by a low G + C content (~36%). Notably, they lack structural protein genes V and IX, as well as homologs of the mastadenoviral early regions E1, E3, and E4 (Davison et al., 2000; Kovács and Benko, 2011).

The first identified siadenovirus is turkey adenovirus 3 (TAdV-3), also known as turkey hemorrhagic enteritis virus (THEV). It causes hemorrhagic enteritis, an acute gastrointestinal disease that primarily affects turkeys aged 6–11 weeks, and markedly impairs both cellular and humoral immune responses in the host (Dhama et al., 2017; Musa et al., 2024). THEV-infected turkeys exhibit increased susceptibility to secondary bacterial infections, notably those caused by *Escherichia coli* and *Clostridium perfringens* (the primary agent of necrotic enteritis) (Musa et al., 2024).

Currently, the quail industry ranks as the third-largest in the global poultry sector, and its breeding segment has been experiencing steady expansion (Liu et al., 2024). However, many diseases still pose a significant threat to the quail industry, including viral and bacterial pathogens. Ulcerative enteritis (also known as quail disease) exerts a serious impact on the quail industry, which was considered to be caused by a Gram-positive anaerobic spore-forming bacillus, and can lead to mortality rates up to 100% (Davis et al., 1971; Berkhoff et al., 1974) and *Clostridium colinum, Clostridium perfringens*, *Clostridium sordellii* were found to be associated with this disease (Shivaprasad et al., 2008; Crespo et al., 2013).

In May 2024, an outbreak of ulcerative enteritis-like disease associated hemorrhagic enteropathy occurred in a layer quail farm that raises 180,000 yellow-feathered quail (*Coturnix japonica*) in Shaoguan City, Guangdong Province, China (Supplementary Fig. S1). One to two hundred of quail died every day due to unknown causes, and antibiotic administration showed no effect. Six pooled tissue samples from six diseased quail, including small intestines, liver, spleen, heart, and lungs, were collected by a local veterinarian and shipped on ice to our laboratory to screen for possible causative agent(s). After arrival, the samples were stored at −80 °C until use.

No PCR positive results were obtained using the virus-detection primers for Newcastle disease virus, fowl adenovirus, Marek's disease virus, infectious bursal disease virus, Tembusu virus, infectious bronchitis virus, astrovirus, avian influenza virus, circoviruses and avian reovirus, as we did in previous experiment (Liao et al., 2023, 2025) (Supplementary Table S1).

Next-generation sequencing (NGS) on the Illumina HiSeq × 10 platform was then carried out using nucleic acids of the samples. The

* Corresponding author.
E-mail addresses: xiaocht@126.com, xiaocht@hnu.edu.cn (C.-T. Xiao).
Peer review under the responsibility of editorial board of *Virologica Sinica*.
[1] Hui Tang and Yin Shi contributed equally to this work.

https://doi.org/10.1016/j.virs.2026.04.002
Received 13 December 2025; Accepted 7 April 2026
Available online 10 April 2026

complete genome was successfully obtained by assembling of the contigs generated from NGS and the sequencing results of PCRs using primers designed to amplify the gaps between the contigs (Supplementary Table S2). The genome of this virus, designated as quail adenovirus 1 (QAdV-1)-HNU-SGX-2024, is 26,113 base pairs (bp) in length, with a G + C content of 32.7%, which exhibits a genome organization similar to that of THEV and other members of the genus *Siadenovirus* (Fig. 1A).

Inverted terminal repeats (ITRs) of 39 bp were identified at both ends of the strain HNU-SGX-2024 genome, which were of the same length as those of THEV. Twenty-eight open reading frames (ORFs) were predicted in the genome of HNU-SGX-2024, and their sizes as well as identities with the corresponding ORFs of the reference THEV (NC_001958) are listed in Supplementary Table S3. The genome of QAdV-1 shared 54%–74.4% identities with the genomes of other known siadenoviruses available in GenBank. The DNA polymerase (Pol) consists of 1112 amino acids. BLAST analysis and sequence comparisons revealed that it showed 51.1%–76.3% identity with the Pol proteins of the other siadenoviruses, with the highest identity of 76.3% observed with the Pol protein of THEV (NC_001958). According to the species demarcation framework established by the International Committee on Taxonomy of Viruses (ICTV), adenovirus species designation is based on the concordant evaluation of multiple criteria, including phylogenetic distance, host range, nucleotide composition, and genome organization. Specifically, species assignment requires support from at least two of these characteristics, with phylogenetic divergence typically exceeding 10%–15% in maximum likelihood analyses of the Pol amino acid sequence. In this context, strain HNU-SGX-2024 exhibits a distinct phylogenetic position relative to recognized siadenovirus species, exceeding the accepted Pol amino acid divergence threshold, and infects a novel host species, quail. Together, these features support its classification as a novel siadenovirus species within the genus *Siadenovirus*. Accordingly, the virus has been provisionally designated *Siadenovirus coturnicis*, following the ICTV recommendations for the formation of Latinized binomial virus species names (Postler et al., 2022), and has been proposed to the ICTV as a novel species (https://ictv.global/report/chapter/adenoviridae/adenoviridae/siadenovirus).

To infer the genetic relationship between HNU-SGX-2024 and other *siadenovirus* strains, as well as selected representative fowl aviadenovirus (FAdV) strains from China, phylogenetic analyses were conducted with the amino acid sequences of the Pol protein and the complete genomes. In both phylogenetic trees, HNU-SGX-2024 formed a distinct, independent clade separate from other known *siadenovirus* strains but clustered closely with the THEV (TAdV3) clade (Fig. 1B and C).

To quantify the virus loads in the samples, a set of Taqman realtime PCR (qPCR) procedures was established with the primers (QAdV-DF/DR) and the probe (QAdV-prob) targeting the *sialidase* gene designed based on the genome of the present QAdV-1 strain (Supplementary

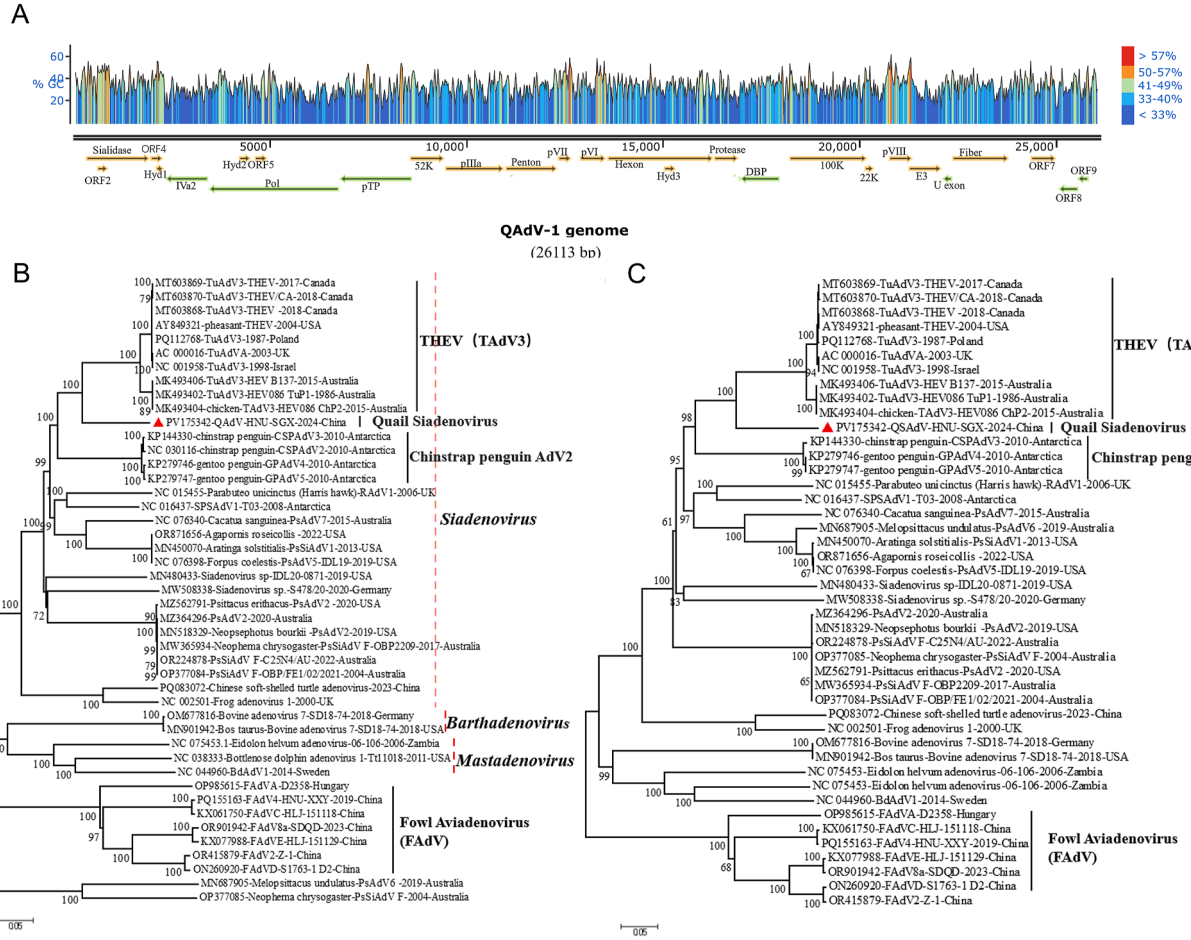

Fig. 1. The genomic feature and phylogenetic analyses of the present quail Siadenovirus (QAdV-1). **A** Schematic illustration of the predicated ORFs in the genome of the present quail Siadenovirus (QAdV-1). The genome is marked at 5-kb intervals. Arrows, proportional in size, denote individual ORFs. The G + C content of the genome is shown above. The ORFs are listed in Supplementary Table S3. **B** and **C** The evolutionary trees constructed based on the genomes (**B**) and the amino acid sequences of DNA polymerase (Pol) (**C**) of the present quail siadenovirus and those siadenoviruses available in GenBank. The phylogeny was inferred using the Maximum Likelihood method in MEGA7. The quail siadenovirus strain HNU-SGX-2024 characterized in the present study is marked with red triangle. The genera of *Siadenovirus*, *Barthadenovirus* and *Mastadenovirus* are indicated with red dashed lines.

Table S2). The standard curve of the qPCR in the present study was y = −3.331x+41.5 (x: log value of virus copy number in the reaction; y: CT value of qPCR in the reaction), with a correlation coefficient $R^2 = 0.997$, and the lowest detectable viral copy number per reaction was 10.

An attempt to isolate the potential virus in the sample using the chicken embryo fibroblast cell line (DF-1) failed, as no cytopathic effect (CPE) was observed after 5 passages, and no virus was detected in the cell cultures by PCR using the present primers (Supplementary Table S1). Nine-day-old specific-pathogen-free (SPF) and 7-day-old commercial quail embryos were also used to isolate the potential virus by inoculating 100 μL of 0.22 μm-filtered freeze-thaw supernatants of the tissue homogenates into the allantoic cavity via standard procedures. In the collected allantoic fluids, low viral titers with CT values from 32.1 to 38.1 were observed in chicken embryos, demonstrating very limited or no replication of QAdV-1 in these chicken embryos. Slightly higher viral titers with CT values from 28.4 to 36.1 were detected in allantoic fluids of quail embryos, also indicating a limited growth of the virus in these quail embryos. No other viruses were detected in the allantoic fluids by PCR using the present detecting primers (Supplementary Table S1).

Although the attempt to isolate the virus failed, a preliminary infection study was performed on quail and chicks to test the pathogenicity and the potential for cross-species transmission. The infected quail exhibited a mortality rate of 50% (8/16; Fig. 2A) and the virus was detected in their fecal swabs from 3 days post-infection (DPI) onward, and this detection persisted until 78 DPI when the experiment was terminated (Fig. 2B). The average viral titer in the fecal swabs of the infected group exhibited an upward trend until 72 DPI; notably, higher viral loads (ranging from $10^{6.1}$ to $10^{7.0}$ viral genome equivalents per swab, on average) were observed after 66 DPI (Fig. 2B).

On necropsy, in some individuals, the contents of the duodenum, jejunum and ileum were black, and the cecum was either black or yellow (Supplementary Fig. S2B, C and F); extensive hyperemia or hemorrhage was observed in the small intestine (Supplementary Fig. S2B and C), and white urate contents were found in the cloaca (Supplementary Fig. S2D); mucosal hyperemia was evident in the proventriculus (Supplementary Fig. S2A) and white striated contents could be found in the bursa of Fabricius (Supplementary Fig. S2E); the heart appeared edematous, soft and pale (Supplementary Fig. S2G), and the spleen turned pale with hemorrhagic spots (Supplementary Fig. S2H). The virus could be

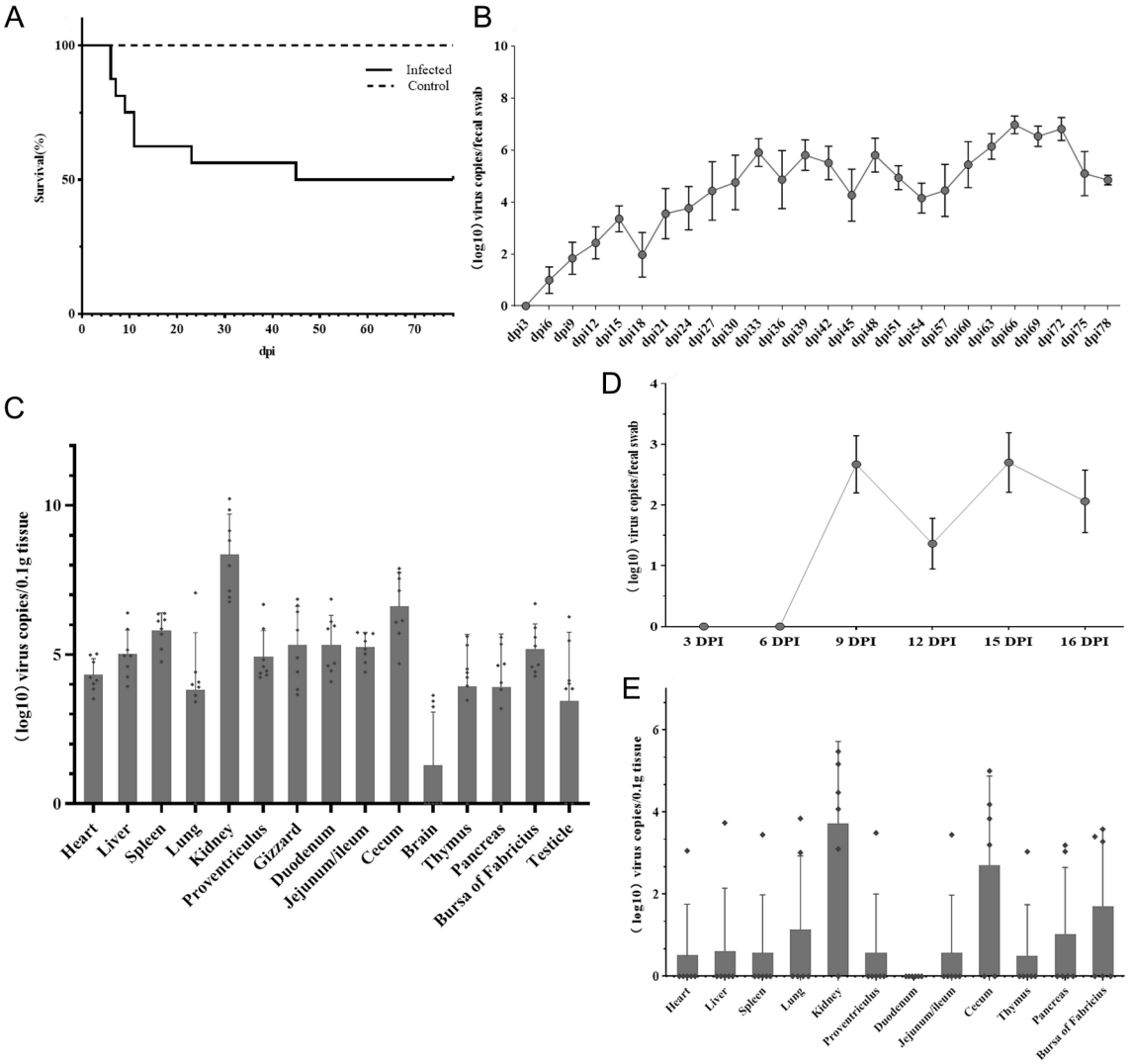

Fig. 2. Challenge data of QAdV-1 in quails and chicks. **A** Survival rates of quail inoculated with tissue homogenates containing QAdV-1 HNU-SGX-2024. The infected group was monitored daily for 78 days after infection. **B** Viral shedding in the fecal swabs of quail orally and subcutaneously inoculated with tissue homogenates containing QAdV-1 HNU-SGX-2024. Values are expressed as mean viral copy number ± standard error. **C** The virus titers in various organs of the quail experimentally infected with homogenates containing QAdV-1. Error bars representing the standard deviation are shown above the boxes. **D** Viral shedding in the fecal swabs of SPF chicken infected with homogenates containing QAdV-1. Values are expressed as mean viral copy number ± standard error. **E** The virus titers in various organs of SPF chicken infected with homogenates containing QAdV-1. Error bars representing the standard deviation are shown above the boxes.

detected in various organs of the infected quail, with the highest titers found in tissues of the kidney, cecum, bursa of Fabricius, spleen, and duodenum, while the titer in the brain tissue was the lowest (Fig. 2C). Notably, the highest viral copies were found in the kidney, with a CT value of 13.8, approximately equal to $10^{10.2}$ viral genome equivalents per 0.1 g of tissue.

However, no obvious symptoms were observed in the infected chicks and no birds died, although QAdV-1 was detected in fecal swabs from 9 DPI on, with viral loads ranging from undetected to $10^{5.5}$ viral genome equivalents per swab (Fig. 2D). On necropsy, 5 out of the 16 chicks had a swollen and dark cecum, with a congested jejunum and ileum (Supplemental Fig. S3). A high viral titer was found in the kidney, cecum and bursa of Fabricius (Fig. 2E). However, in general, the viral titers in both the fecal swabs and the tissues were significantly lower than those in the quail.

In hematoxylin and eosin (H&E)-stained sections, microscopic lesions were observed in the organs of infected quail. In the kidney tissue, renal hemorrhage, inflammatory cell infiltration, and indistinct renal tubular structures were noted (Supplementary Fig. S4A). In the cecum, the mucosa and submucosa showed extensive inflammatory cell infiltration, irregular mucosal gland architecture, and swelling/degeneration of glandular epithelial cells (Supplementary Fig. S4B). The duodenum exhibited villous atrophy and shortening with apical fusion, along with swollen/degenerated intestinal epithelial cells showing partial exfoliation. Scattered or small focal aggregates of dark blue-stained inflammatory cells were observed in both the mucosal and submucosal layers (Supplementary Fig. S4C). Similar changes were detected in the ileal tissue (Supplementary Fig. S4D). Eosinophilic inclusion bodies were seen across various tissues (some indicated by arrows in Supplementary Fig. S4). IHC staining with the mouse polyclonal antibody serum prepared in the present study showed viral antigen-positive signals (brown deposits) in the kidney (Supplementary Fig. S4E) and cecal tissues (Supplementary Fig. S4F). No significant histologic lesions were observed in the mock-infected quail (data not shown).

Interestingly, four amino acids mutations were detected in the Pol protein of the virus, which is ^{145}Y and ^{149}D^{150}I^{151}P in the Pol protein before challenge and they were changed to ^{145}N and ^{149}S^{150}N^{151}S after animal experiment. However, although three of the substitutions (Y145 N, I150S, P151S) alter the polarity of the amino acids, they do not cause obvious structural change, as predicted by Alphafold (https://alphafoldserver.com/) (Supplementary Fig. S5). Further studies are needed to investigate the cause of the mutations and the possible effect of these substitutions on the replication or pathogenicity of the virus.

Collectively, a novel quail siadenovirus (QAdV-1), with the species name designated as *Siadenovirus coturnicis,* was first identified in diseased quail. Pilot animal challenge studies indicated that the virus could be detected at high titers in various organs of quail and that it may be pathogenic to quail. Cross-species transmission to chicks was also observed, although viral titers in chicks were significantly lower and no mortalities occurred. Given its close genetic relationship with THEV, great attention should be paid to its potential role in the immunosuppression, similar to that of THEV, as it may pose a significant threat to the poultry industry, especially the quail industry. Further investigations, including isolating QAdV-1 in various cell types (particularly quail-derived ones), constructing infectious clones, exploring its potential immunosuppressive mechanisms, and developing vaccines, are needed to elucidate QAdV-1 pathogenicity and develop prevention strategies.

FOOTNOTES

This work was supported by the National Natural Science Foundation of China, China (Grant No. 32272975), and Hunan Science and Technology Innovation Plan 2025ZYJ003. The authors declare that they have no conflict of interest. The mouse, quail and chicken infection experiments described in this study were approved by the Animal Care and Use Committee of Hunan University, China (approval no. HNUBIO202402003) and conducted using humane procedures. The genome of QAdV-1 has been deposited in GenBank under the accession number PV175342 and has also been deposited in ScienceDB (https://doi.org/10.57760/sciencedb.v.00014). Supplementary data to this article can be found online at https://doi.org/10.1016/j.virs.2026.04.002.

REFERENCES

Benko, M., Aoki, K., Arnberg, N., Davison, A.J., Echavarría, M., Hess, M., Jones, M.S., Kaján, G.L., Kajon, A.E., Mittal, S.K., Podgorski, I.I., San Martín, C., Wadell, G., Watanabe, H., Harrach, B., Consortium, I.R., 2022. ICTV virus taxonomy profile: *adenoviridae* 2022. J. Gen. Virol. 103, 001721.

Berkhoff, G.A., Campbell, S.G., Naylor, H.B., Smith, L.D., 1974. Etiology and pathogenesis of ulcerative enteritis ("quail disease"). Characterization of the causative anaerobe. Avian Dis. 18, 195–204.

Crespo, R., Franca, M., Shivaprasad, H.L., 2013. Ulcerative enteritis-like disease associated with in quail. Avian Dis. 57, 698–702.

Davis, R.B., Brown, J., Dawe, D.L., 1971. Quail–biological indicators in the differentiation of ulcerative and necrotic enteritis of chickens. Poult. Sci. 50, 737–740.

Davison, A.J., Wright, K.M., Harrach, B., 2000. DNA sequence of frog adenovirus. J. Gen. Virol. 81, 2431–2439.

Dhama, K., Gowthaman, V., Karthik, K., Tiwari, R., Sachan, S., Kumar, M.A., Palanivelu, M., Malik, Y.S., Singh, R.K., Munir, M., 2017. Haemorrhagic enteritis of turkeys - current knowledge. Vet Quart 37, 31–42.

Harrach, B., Tarján, Z.L., Benkő, M., 2019. Adenoviruses across the animal kingdom: a walk in the zoo. FEBS Lett. 593, 3660–3673.

Kovács, E.R., Benko, M., 2011. Complete sequence of raptor adenovirus 1 confirms the characteristic genome organization of siadenoviruses. Infect. Genet. Evol. 11, 1058–1065.

Liao, J.Y., Tang, H., Xiong, W.J., Liu, T.N., Li, J.Y., Xia, J.Y., Xiao, C.T., 2023. Isolation and characterization of a novel goose ovaritis-associated cluster 3 tembusu virus. Poult. Sci. 102, 102867.

Liao, J.Y., Shi, Y., Tang, H., Fu, P., Li, J.Y., Zhang, Y.S., Wu, Q., Peng, Y.S., Xiao, C.T., 2025. Emerging and characterization of a novel fowl adenovirus 4 strain with open reading frame 19 (orf19) in diseased chickens from China. Poult. Sci. 104, 104702.

Liu, Y., Song, M.X., Bai, H., Wang, C.H., Wang, F., Yuan, Q., 2024. Curcumin improves the egg quality, antioxidant activity, and intestinal microbiota of quails during the late laying period. Poult. Sci. 103, 103233.

Musa, L., Rapi, M.C., Franciosini, M.P., Lupini, C., Catelli, E., Addis, M.F., Grilli, G., 2024. Turkey hemorrhagic enteritis (the): a short overview. Pathogens 13, 663.

Postler, T.S., Rubino, L., Adriaenssens, E.M., Dutilh, B.E., Harrach, B., Junglen, S., Kropinski, A.M., Krupovic, M., Wada, J., Crane, A., Kuhn, J.H., Mushegian, A., Rumnieks, J., Sabanadzovic, S., Simmonds, P., Varsani, A., Zerbini, F.M., Callanan, J., Draper, L.A., Hill, C., Stockdale, S.R., 2022. Guidance for creating individual and batch latinized binomial virus species names. J. Gen. Virol. 103, 001800.

Shivaprasad, H.L., Uzal, F., Kokka, R., Fisher, D.J., McClane, B.A., Songer, A.G., 2008. Ulcerative enteritis-like disease associated with Clostridium perfringens type a in bobwhite quail (Colinus virginianus). Avian Dis. 52, 635–640.